

UNIVERSITÀ DEGLI STUDI DI PADOVA

DIPARTIMENTO DI FISICA E ASTRONOMIA G.GALILEI

CORSO DI LAUREA TRIENNALE IN  
FISICA

# Quantum optimal control of two-qubit gates in Rydberg atoms

*Relatore:*

PROF. SIMONE MONTANGERO

*Laureando:*

MARCO DALL'ARA

1217301

Anno Accademico 2021/2022



## **Abstract**

Quantum computers promise to outperform conventional computational processes by taking advantage of exclusive quantum properties, such as superposition and entanglement. In the last years, several breakthroughs have demonstrated Rydberg atoms as a promising scalable quantum computing platform. Rydberg atoms are arrays of identical neutral atoms trapped in optical tweezers, where two different internal states of the atom encode a qubit with long coherence times. The progress in manipulating individual Rydberg atoms has allowed the experimental realization of single and two-qubit gate protocols. This has motivated a widespread theoretical interest in improving gate fidelity and finding alternative protocols. After reviewing the physics of Rydberg atoms and the most up-to-date gate protocols, in this thesis we simulate one and two qubits gates, then we apply optimal control techniques, as implemented in the open-source optimal control suite QuOCS, to optimize the laser pulse shapes for the realization of controlled-phase gate.



# Indice

<b>1</b>	<b>Introduction</b>	<b>1</b>
<b>2</b>	<b>Rydberg atoms</b>	<b>3</b>
2.1	General proprieties . . . . .	3
2.2	Lifetime . . . . .	4
2.3	Rydberg-Rydberg interaction . . . . .	5
2.4	Light-Atom interaction . . . . .	6
2.5	Rydberg blockade . . . . .	8
2.6	optical tweezers . . . . .	10
<b>3</b>	<b>Quantum optimal control</b>	<b>11</b>
3.1	Control problems in Quantum Computing . . . . .	12
3.2	Pulse shaping and QSL . . . . .	12
3.3	Crab and dCrab Algorithms . . . . .	12
<b>4</b>	<b>Gate protocols and simulations</b>	<b>13</b>
4.1	Single-qubit gate . . . . .	13
4.2	Two-qubit gate . . . . .	13
4.3	Simulation of a CZ gate . . . . .	13
<b>5</b>	<b>Conclusion</b>	<b>15</b>
<b>6</b>	<b>Immagini e Tabelle</b>	<b>17</b>
6.1	Immagine singola . . . . .	17
6.2	Immagine multipla . . . . .	18
6.3	Tabelle . . . . .	18
<b>7</b>	<b>Formule</b>	<b>19</b>

<b>8 Pseudocodice e codice</b>	<b>21</b>
8.1 Pseudocodice . . . . .	21
8.2 Codice . . . . .	21
<b>Bibliografia</b>	<b>23</b>

# Capitolo 1

## Introduction

La struttura utilizzata in questo template non è obbligatoria, però ritengo che sia molto comoda per evitare di scrivere file troppo lunghi e di avere un controllo migliore sulla struttura. Questa prevede di scrivere l'introduzione al capitolo in un file salvato nella cartella principale e di sviluppare le sezioni all'interno di una cartella. Esempio di richiamo ad un riferimento .

1/2 Pagine





# Capitolo 2

## Rydberg atoms

Neutral atom systems provide important features for the realization of quantum computers: optical pumping can be used to prepare initial states, handy interactions are possible with microwaves and precise measurements can be made using fluorescence. Any atom (or even molecule) in a state with a valence electron highly-excited, i.e. with a large principal quantum number  $n$  of the order of tens or hundreds is defined as a Rydberg atom. The flexibility of controlling interactions is achievable thanks to huge dipole matrix elements which also make possible features like Rydberg Blockade. The latter is the phenomenon that prevents the simultaneous excitation of more than an atom in a certain volume to a state with a large  $n$  (Rydberg state), making the entangling of qubits possible. Thanks to the possibility of trapping these atoms in optical tweezers we can reduce their intrinsic instability in a non-isolated system, caused by small ionization energies. Optical tweezers systems and a radiative lifetime that scales with  $n$  make long decoherence times possible.

### 2.1 General proprieties

We expect that the orbit size  $\langle r \rangle$  scales with  $n^2$  we can think of our atom as if all the electrons of the inner states perfectly shield the nucleus. So, if the atom is neutral, we can in first approximation, consider it as a Hydrogen one. To have a better agreement with experiments we could make weaker approximations taking into consideration the fine structure corrections and quantum defect theory, in such a way to consider the ionic core not as a point charge, relativistic effects, and spin-orbit interaction. The final eigenvalues are  $E_{n,l} = E_{nl} + \Delta E_{fs}$  where according to the fine structure correction we have (citation book atomic physics)

:

$$\Delta E_{fs} = -E_{n,l} \frac{\alpha^2}{n^2} \left[ \frac{n}{j + 1/2} - \frac{3}{4} \right] \quad (2.1)$$

and due to the quantum defect theory :

$$E_{n,l} = -\frac{R_\infty}{1 + \frac{m_e}{M}} \frac{1}{(n - \delta_{n,l})^2} \quad (2.2)$$

where  $n$  is the principal quantum number,  $l$  is the azimuthal quantum number,  $\alpha$  is the fine structure constant,  $R_\infty$  is the Rydberg constant,  $m_e$  is the mass of the electron,  $M$  is the total mass of the atom,  $j$  is the total angular momentum quantum number and  $\delta_{n,l}$  is the quantum defect which depends on the atomic species and on  $n$  and  $l$ . The latter correction could be intuitively interpreted in a semi-classical view as illustrated in Fig.2.1(a). Is important to underline that the approximation of the Hydrogen atom is mostly valid for large  $l$ (2.1(b)).

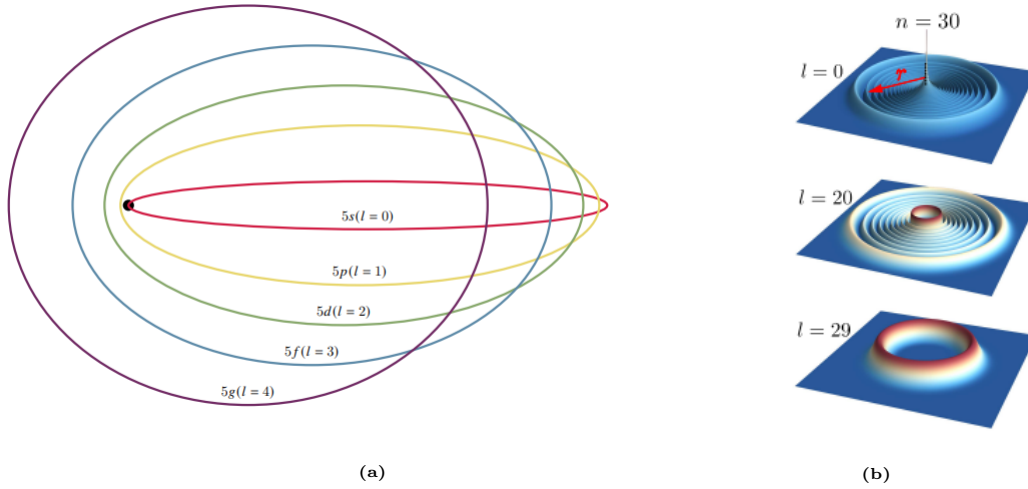


**Figura 2.1:** (a) Semiclassical orbiting of the valence electron around the atomic core (black dot), with  $l$  values of orbital angular momentum. (b) Density distributions of the valence electron in the radial direction of 87Rb (cita bibblbio). When  $l=n-1$  this electron is highly localized around  $n^2 a_0$  as the hydrogen atom.

## 2.2 Lifetime

Rydberg atoms are mostly unstable and as we'll see their decay is the biggest source of quantum gate infidelity. Their lifetime  $\tau$  has essentially two contributes:

$$\frac{1}{\tau} = \frac{1}{\tau_0} + \frac{1}{\tau_{bb}} \quad (2.3)$$

**Radiative lifetime  $\tau_0$** 

The physical mechanism that dominates this process is the spontaneous emission due to vacuum electromagnetic field fluctuations at 0° K. Given a state  $n$ , the transition rates for spontaneous emission  $1/\tau_0$  is the sum of the Einstein coefficients all over the possible lower final state  $n'$ . In a classical electrodynamics view we would expect that  $1/\tau_0 \propto 1/n$  since the bigger is his quantum principle number, the farther an electron is from the nucleus, the smaller the acceleration it experiences and therefore the radiation rate. In particular, it can be shown that the radiative lifetime scale as  $n^5$  for transition to neighboring Rydberg states or as  $n^3$  for final low-energy states.

**Blackbody lifetime  $\tau_{bb}$** 

This term pops up when considering a non-zero Temperature environment and it's due to the interaction between the atom and blackbody radiation of temperature  $T$ . This term is dominant over the radiative lifetime since Rydberg states have low-frequency transitions and large electric dipole moments between each other. The BBR is thus strongly coupled to the transition between Rydberg states and the BBR term of lifetime  $\tau_{bb}$  scales as  $n^2$ . Blackbody lifetime for transition to low energy states is negligible.

For example, taking  $^{87}\text{Rb}$  atom at  $T=300\text{K}$  and  $n \approx 50$  the total lifetime is 50 microsec so to manipulate them are needed frequencies of the order of MHz.

## 2.3 Rydberg-Rydberg interaction

If the interatomic distance of two Rydberg Atoms is much greater than the Rydberg state radius, we can regard our atoms as electric dipoles with  $\mathbf{p} = -e\mathbf{d}$ , where  $\mathbf{d}$  is the displacement of the electron from the cation. Then atoms interaction reduces to a dipole-dipole interaction :

$$V_{dd} = \frac{e^2}{4\pi\epsilon_0} \frac{\mathbf{d}_1 \cdot \mathbf{d}_2 - 3(\mathbf{d}_1 \cdot \hat{\mathbf{u}}_R)(\mathbf{d}_2 \cdot \hat{\mathbf{u}}_R)}{|\mathbf{R}|^3} \quad (2.4)$$

where  $\mathbf{R}$  is the interatomic distance and  $\hat{\mathbf{u}}_R$  the versor along  $\mathbf{R}$ .

Without an electric field, it is easy to show that  $\langle \mathbf{d} \rangle = 0$  since for each eigenvector we have (we indicate with  $|1\rangle$  the general eigenvector  $|\Psi_{nlm}\rangle$  and with  $\hat{P}$  the parity operator)

$$\begin{aligned} \langle \mathbf{d} \rangle_{nlm} &:= \langle \Psi_{nlm} | \mathbf{d}(t) | \Psi_{nlm} \rangle = \langle \Psi_{nlm}(t) | \mathbf{d} | \Psi_{nlm}(t) \rangle = \langle \Psi_{nlm} | \mathbf{d} | \Psi_{nlm} \rangle = \\ &\langle \Psi_{nlm} | \hat{P} \hat{P}^{-1} \mathbf{d} \hat{P} \hat{P}^{-1} | \Psi_{nlm} \rangle = \langle \Psi_{nlm} | \hat{P}(-\mathbf{d}) \hat{P}^{-1} | \Psi_{nlm} \rangle = - \langle \mathbf{d} \rangle_{nlm} \end{aligned}$$

and then  $\langle \mathbf{d} \rangle = 0$  which involves that  $\langle V_{dd} \rangle = 0$ .

Beside that,  $\mathbf{d}$  has non-zero matrix elements between states with different parities so it can be shown that (citazione cinese paper), in the case of a single transition from  $|r_1\rangle |r_2\rangle$  to  $|r'_1\rangle |r'_2\rangle$  we can reduce the description in an Hamiltonian in the subspace  $\{|r_1, r_2\rangle, |r'_1, r'_2\rangle\}$ :

$$\hat{H} = \begin{bmatrix} 0 & C_3/R^3 \\ C_3/R^3 & \delta_F \end{bmatrix} \quad (2.5)$$

where  $C_3 \propto n^4$  is the anisotropic interaction coefficient and  $\delta_F = (E_{r'_1} + E_{r'_2}) - (E_{r_1} + E_{r_2})$  the Foster defect. In the case where  $\delta_F \gg V(R) := C_3/R^3$  we could treat the system with perturbation theory getting as a result  $\Delta E_{\pm} = \pm C'_6/R^6$  with  $C'_6 = C_3^2/\delta_F$ . Note that, since  $\langle V_{dd} \rangle = 0$  we need to consider second-order corrections.

In general, fixing  $r'_1 = r'_2 = r$ , we can generalize and consider all the second-order perturbations of others Rydberg states:

$$C_{rr} = \sum_{|r_1, r_2\rangle} \left[ \frac{C_3^2}{R^6 \delta_F} \right]_{|r, r\rangle \rightarrow |r_1, r_2\rangle} = \sum_{|r_1, r_2\rangle} \frac{|\langle r_1, r_2 | V_{dd} | r, r \rangle|^2}{2E_r - E_{r_1} - E_{r_2}} = C_{6,rr}/R^6 \quad (2.6)$$

This is the so-called Van der Waals interaction and we will consider that as the Rydberg-Rydberg interaction in the next chapters. The  $C_{6,rr}$  coefficient scales as  $n^{11}$  which shows the possibility of huge interactions between Rydberg atoms.

## 2.4 Light-Atom interaction

Considering a single atom with two possible states,  $|g\rangle$ ,  $|e\rangle$ , and the light as an oscillating electric field (monochromatic plane wave)  $\mathbf{E}(t) = \mathbf{E}'_0 \cos(\omega t +$

$\phi) = \mathbf{E}_0 e^{-i\omega t} + \mathbf{E}_0^* e^{i\omega t}$  with  $\mathbf{E}_0 = \mathbf{E}'_0 e^{i\phi}/2$ , the interaction between them can be modellized as

$$\hat{H}_{int} = -\mathbf{p} \cdot \mathbf{E}(t) \quad (2.7)$$

where  $\mathbf{p}$  is the electric dipole of the atom. In fact we are considering our atom a dipole and we are neglecting higher multipole terms since their smaller contributes. As we have already seen the dipole operator has only non-diagonal term different by zero so we could write the Hamiltonian of our two level system with the interaction of dipole with light:

$$\hat{H}_{int} = -\hbar(\Omega e^{-i\omega t} + \hat{\Omega} e^{i\omega t}) |g\rangle \langle e| - \hbar(\hat{\Omega}^* e^{-i\omega t} + \Omega^* e^{i\omega t}) |e\rangle \langle g| \quad (2.8)$$

with  $\Omega_0 = \hbar^{-1} \langle e | \mathbf{p} | g \rangle \cdot \mathbf{E}'_0$  the Rabi frequency,  $\Omega = -\frac{\Omega_0}{2} e^{-i\phi}$  and  $\hat{\Omega} = -\frac{\Omega_0}{2} e^{i\phi}$ . Defining  $\omega_d := \omega_{|e\rangle} - \omega_{|g\rangle}$  we can express the hamiltonian of the non-interacting system as  $\hat{H}_0 = -\hbar\omega_d/2 |g\rangle \langle g| + \hbar\omega_d/2 |e\rangle \langle e|$  since the difference of the two eigenvalues of the energies are  $\Delta E = E_e - E_g$ . The total hamiltonian is then:

$$\hat{H} = -\hbar\omega_d/2 |g\rangle \langle g| + \hbar\omega_d/2 |e\rangle \langle e| - \hbar(\Omega e^{-i\omega t} + \hat{\Omega} e^{i\omega t}) |g\rangle \langle e| - \hbar(\hat{\Omega}^* e^{-i\omega t} + \Omega^* e^{i\omega t}) |e\rangle \langle g| \quad (2.9)$$

If we consider a unitary transformation to the Dirac picture and small detuning  $\Delta := \omega - \omega_d \ll \omega_d + \omega$  we reach:

$$\hat{H}_{int,dirac} = -\hbar(\Omega e^{-i\Delta t} + \hat{\Omega} e^{i(\omega_d+\omega)t}) |g\rangle \langle e| - \hbar(\hat{\Omega}^* e^{-i(\omega_d+\omega)t} + \Omega^* e^{i\Delta t}) |e\rangle \langle g| \quad (2.10)$$

$$\approx -\hbar(\Omega e^{-i\Delta t}) |g\rangle \langle e| - \hbar(\Omega^* e^{i\Delta t}) |e\rangle \langle g|$$

The latter is the so-called Rotating wave approximation (cita immagine wiki). Finally transforming back to the Schrodinger picture and going in a rotating frame of reference defined by  $\hat{H}_{rwf} = \hat{U} \hat{H} \hat{U}^\dagger + i\hbar \frac{\partial \hat{U}}{\partial t} \hat{U}^\dagger$  with

$$\hat{U} = \begin{bmatrix} e^{-i\omega t/2} & 0 \\ 0 & e^{i\omega t/2} \end{bmatrix} \quad (2.11)$$

we have the final hamiltonian:

$$\hat{H} = -\hbar\Delta/2 |g\rangle \langle g| + \hbar\Delta/2 |e\rangle \langle e| + \hbar(\Omega |e\rangle \langle g| + \Omega^* |g\rangle \langle e|) \quad (2.12)$$

Note that we have considered a fixed point for the electric wave. Considering a more realistic system is possible to take into account the spacial term even considering a Gaussian incident beam instead of a harmonic plane wave.

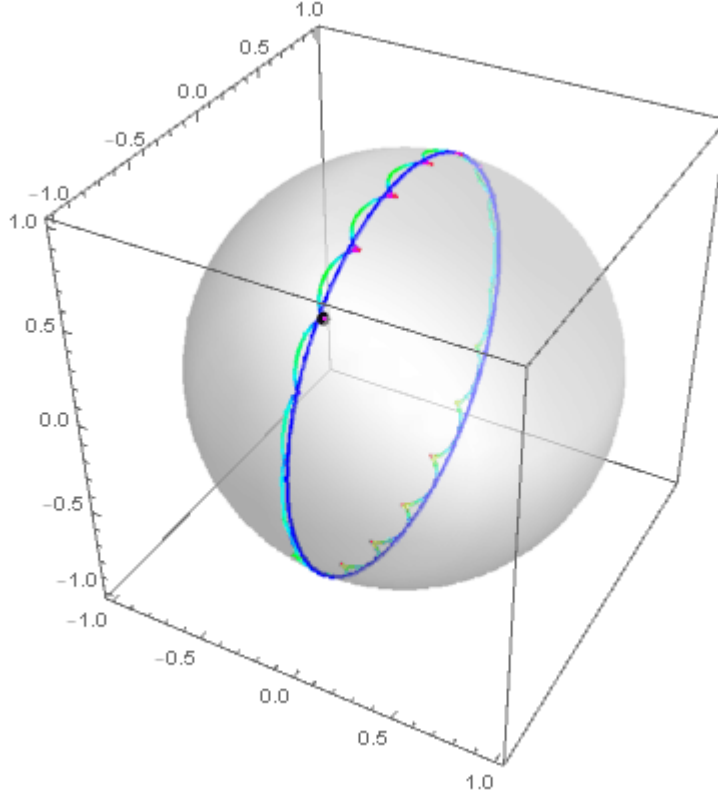


**Figura 2.2:** When the Detuning is small, the term  $e^{i\omega+\omega_d}$  oscillates much faster and thus is negligible. In green, we don't apply the RWA, while in blue we do.

## 2.5 Rydberg blockade

Let's consider now two identical Rydberg atoms interacting with light, where each one have a basis composed by  $|g\rangle$ ,  $|r\rangle$  (ground and a singular Rydberg state). In particular, with light we intend a resonant laser (without detuning) which couples  $|g\rangle$  to  $|r\rangle$ . Due to Rydberg-Rydberg interaction, we cannot promote both atoms as the first excited shifts the Rydberg energy levels of the other atom off-resonance. Because we are using resonant light, we shrink the Rydberg states only to  $|r\rangle$ , but we don't neglect the interaction of all Rydberg states with the only one reachable.

The dynamics is governed by the following Hamiltonian:

$$\hat{H} = \hbar(\Omega |r\rangle \langle g| \otimes \mathbb{1} + \Omega \mathbb{1} \otimes |r\rangle \langle g| + H.c...) - C_{6,rr}/R^6 |rr\rangle \langle rr| \quad (2.13)$$

We can easily make a change of basis to express the evolution as a three level system with basis  $\{|gg\rangle, |+\rangle = (|gr\rangle + |rg\rangle)/\sqrt{2}, |rr\rangle\}$ :

$$\hat{H} = \hbar\sqrt{2}(\Omega |gg\rangle \langle +| + \Omega |+\rangle \langle rr| + H.c...) - C_{6,rr}/R^6 |rr\rangle \langle rr| \quad (2.14)$$

Note that the term on the left is exactly like the light atom interaction, with a Rabi frequency multiplied by  $\sqrt{2}$ , coupling  $|gg\rangle$  to  $|+\rangle$ . The states  $|+\rangle, |rr\rangle$  are not perfectly coupled since the last term of the hamiltonian could be viewed as the detune term in the light atom hamiltonian(2.12).

### Perfect Blockade

The regime of Perfect Blockade is defined as  $C_{6,rr}/R_b \gg \hbar |\Omega_0|$ , which corresponds to  $R_b := (C_{6,rr}/(\hbar\Omega_0))^{1/6} \gg R$  where  $R_b$  is the blockade radius. As illustrated in the figure 2.3 and as already mentioned we can interpret the Rydberg-Rydberg interaction term as large detune (large because of this regime) and so the  $|rr\rangle$  state is not reachable so it could be discarded from the dynamics.

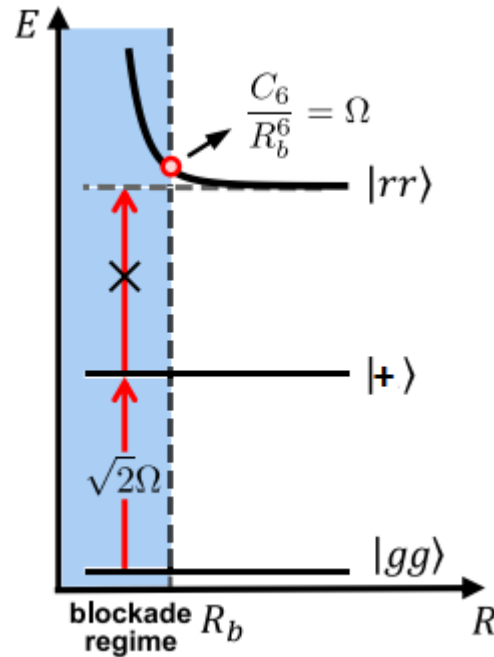


**Figure 2.3:** The Van der Waals interaction shifts out of resonance the state  $|rr\rangle$  if the atoms are separated by  $R < R_b$ .

## 2.6 optical tweezers



## Capitolo 3

# Quantum optimal control

Over the last due decades Quantum Optimal Control has undergone a huge evolution helping the engineering process of quantum physics. This technique in nowadays used from control to quantum many-body physics to Gate optimization, which is one of the most relevant problem for the realization of quantum computers. In general, we search for optimal input parameters which describe some physical interaction in order to achieve a specific objective. As illustrated in figure(schemino) there are mainly two type of optimal control problem: the openloop and the closedloop. In the first one, the analysis is theoretical and implemented in simulations while in the closed loop we deal we the real physical world processing data from experiments and mesurament in order to optimize some input parameters.

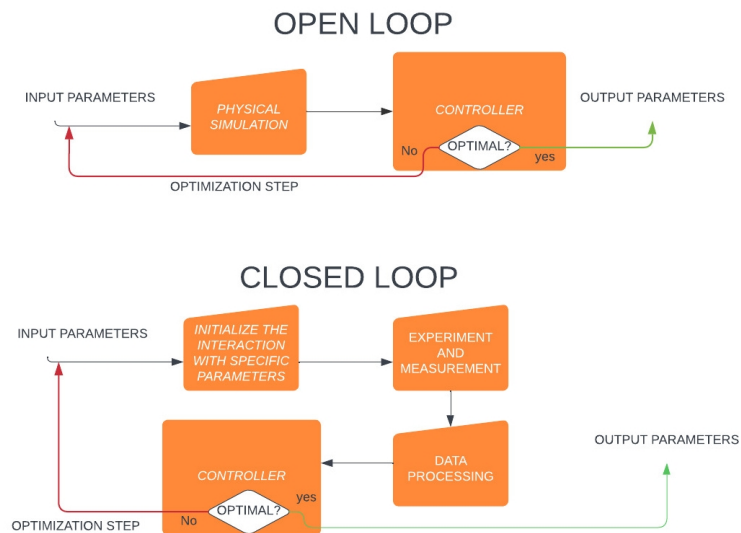


**Figure 3.1:** The two main types types of controls

### 3.1 Control problems in Quantum Computing

1.system dynamics -i.hamiltonians 2.control objective:explain some example 3.control space restrictions(physical constraints): example!

### 3.2 Pulse shaping and QSL

1.pulse shaping problem schemino 2.QSL

### 3.3 Crab and dCrab Algorithms

crab explanation, physical constraints critical points, false traps-i dcrab explanation

# Capitolo 4

## Gate protocols and simulations

5

La struttura utilizzata in questo template non è obbligatoria, però ritengo che sia molto comoda per evitare di scrivere file troppo lunghi e di avere un controllo migliore sulla struttura. Questa prevede di scrivere l'introduzione al capitolo in un file salvato nella cartella principale e di sviluppare le sezioni all'interno di una cartella. Esempio di richiamo ad un riferimento [2].

*«Each thing says what it is...a fruit says 'Eat me'; water says 'Drink me'; thunder says 'Fear me'...»* (Koffka, 1935)

### 4.1 Single-qubit gate

### 4.2 Two-qubit gate

### 4.3 Simulation of a CZ gate



# Capitolo 5

## Conclusion

1 pagina THE END!!!



# Capitolo 6

## Immagini e Tabelle

Metodi più comuni per inserire immagini e esempi di tabelle.

### 6.1 Immagine singola

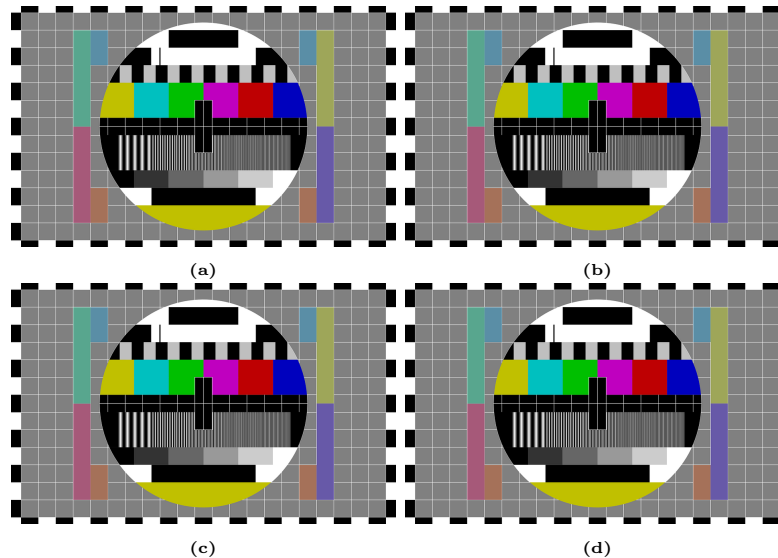
Per fare riferimento ad un immagine, come ad ogni altro elemento a cui viene attribuita una *label* è disponibile il comando *ref*. Riferimento a Figura 6.1.



Figura 6.1: Didascalia

## 6.2 Immagine multipla

Inserire più “sottofigure” in una figura.



**Figura 6.2:** Esempio di figura composta da 4 figure.

## 6.3 Tabelle

Nella seguente tabella vengono mostrati alcuni esempi di separazione delle righe. La separazione delle colonne avviene all’interno delle parentesi grafe dopo il comando *tabular*.

cella1	cella2	cella3
cella4	cella5	cella6
cella7	cella8	cella9
cella10	cella11	cella12

È possibile, inoltre, fissare la dimensione delle colonne.

cella1	cella2	cella3
cella4	cella5	cella6 cella6 cella6 cella6
cella7 cella10	cella8 cella11	cella9 cella12



# Capitolo 7

## Formule

Per inserire delle formule matematiche è possibile utilizzare due metodi:

- in linea: inserendo la formula tra due caratteri \$.
- utilizzando l'ambiente *equation*.

Esempio di formula in linea  $x(t) = x_0 + v_0t + \frac{1}{2}at^2$ .

Esempio di utilizzo dell'ambiente *equation*:

$$x(t) = x_0 + v_0t + \frac{1}{2}at^2 \tag{7.1}$$

Possiamo usare le *label* anche per le equazioni. Legge oraria nell'Equazione 7.1.

Infine, un esempio di formula su più righe:

$$\begin{aligned} x(t) &= x_0 + v_0t + \frac{1}{2}at^2 \\ &= x_0 + v_0t + \frac{1}{2}\frac{F}{m}t^2 \end{aligned} \tag{7.2}$$



# Capitolo 8

## Pseudocodice e codice

In questo template per l’inserimento di pseudocodice è stato utilizzato il pacchetto *algppseudocode*. Per quanto riguarda l’inserimento del codice è possibile utilizzare il comando *verb* per inserire in linea oppure *lstlisting* per inserire blocchi di codice.

### 8.1 Pseudocodice

---

**Algorithm 1** Nome algoritmo

---

**Input:** Input dell’algoritmo

**Output:** Output dell’algoritmo

```
1: variabile  $\leftarrow$  assegnazione valore
2: valore_ritornato  $\leftarrow$  FUNZIONEPROVA(param1, param2)
3: for element in list do
4:   res  $\leftarrow$  DOSOMETHING(element)
5: end for
6: if condizione1 then
7:   do something
8: else if condizione2 then
9:   do something else
10: else
11:   print “Hello World”
12: end if
```

---

### 8.2 Codice

È possibile inserire codice in linea: `print("Hello World")`.

Inoltre è possibile usare l’ambiente *lstlisting* configurando il layout del blocco di

codice nel file *layout.tex*. Il codice può essere importato da un file esterno che metteremo nella cartella *code*.

```
1 # Number of trees in random forest
2 n_estimators = [int(x) for x in np.linspace(start = 100, stop =
    1000, num = 10)]
3 # Number of features to consider at every split
4 max_features = ['log2', 'sqrt']
5 # Maximum number of levels in tree
6 max_depth = [int(x) for x in np.linspace(10, 150, num = 15)]
7 max_depth.append(None)
8 # Minimum number of samples required to split a node
9 min_samples_split = [2, 5, 10]
10 # Minimum number of samples required at each leaf node
11 min_samples_leaf = [1, 2, 4, 6, 8]
12 # Method of selecting samples for training each tree
13 bootstrap = [True, False]
14 random_grid = {'n_estimators': n_estimators,
15                'max_features': max_features,
16                'max_depth': max_depth,
17                'min_samples_split': min_samples_split,
18                'min_samples_leaf': min_samples_leaf,
19                'bootstrap': bootstrap
20                }
21
22 rfc = RandomForestClassifier()
23 rfc_random = RandomizedSearchCV(estimator=rfc,
    param_distributions=random_grid, n_iter=1000, cv=5, verbose=2,
    random_state=3, n_jobs=4)
24
25 rfc_random.fit(df_downsampled, labels_downsampled)
```

Listing 8.1: Didascalia.

# Bibliografia

- [1] Buitinck L., Louppe G., Blondel M., Pedregosa F., Mueller A., Grisel O., Niculae V., Prettenhofer P., Gramfort A., Grobler J., Layton R., Vanderplas J., Joly A., Holt B., Varoquaux G., *API design for machine learning software: Experiences from the scikit-learn project*, 2013.
- [2] *Convolutional Neural Networks*, <http://deeplearning.net/tutorial/lenet.html>, last consultation: 07/01/2020.